

A Time-Freezing Approach for Numerical Optimal Control of Nonsmooth Differential Equations with State Jumps

Armin Nurkanović, Tommaso Sartor, Sebastian Albrecht, Moritz Diehl

Abstract—We present a novel reformulation of nonsmooth differential equations with state jumps which enables their easier simulation and use in optimal control problems without the need of using integer variables. The main idea is to introduce an auxiliary differential equation to mimic the state jump map. Thereby, also a clock state is introduced which does not evolve during the runtime of the auxiliary system. The pieces of the trajectory that correspond to the parts when the clock state was evolving recover the solution of the original system with jumps. Our reformulation results in nonsmooth ordinary differential equations where the discontinuity is in the first time derivative of the trajectory, rather than in the trajectory itself. This class of systems is easier to handle both theoretically and numerically. We provide numerical examples demonstrating the ease of use of this reformulation in both simulation and optimal control. In the optimal control example a single call of a nonlinear programming (NLP) solver yields the same solution as a multi-stage formulation, without the need for exploring the optimal number of stages by enumeration or heuristics.

I. PROBLEM DESCRIPTION

This paper regards the numerical treatment of nonsmooth differential equations in optimal control. The nonsmoothness of $\dot{x}(t) = f(x(t))$ can be classified depending on the classes into which the solution $x(t; x_0)$ and right hand side (r.h.s.) $f(x(t))$ fall: 1) Ordinary Differential Equations (ODE) with nonsmooth but Lipschitz r.h.s. and \mathcal{C}^1 solutions; 2) discontinuous but one-sided Lipschitz r.h.s. with absolutely continuous solutions; 3) solutions that contain state jumps and are functions of bounded variations. This paper focuses on case 3. Since $x(t; x_0)$ jumps, $f(x(t))$ has to contain Dirac- δ impulses. In such cases we cannot in general speak of ODE and we have to use tools such as Measure Differential Inclusions (MDIs) [11]. More compactly, the question is whether a jump discontinuity appears in $x(t; x_0)$ (case 3) or in its first or second time derivative (cases 2 and 1).

This research was supported by the German Federal Ministry of Education and Research (BMBF) via the funded Kopernikus project: SynErgie (03SFK3U0), by the German Federal Ministry for Economic Affairs and Energy (BMWi) via DyConPV (0324166B), and by DFG via Research Unit FOR 2401.

Armin Nurkanović and Sebastian Albrecht are with Siemens Corporate Technology, 81739 Munich, Germany. Armin Nurkanović is also with the Department of Microsystems Engineering (IMTEK) University Freiburg, 79110 Freiburg, Germany {armin.nurkanovic, sebastian.albrecht}@siemens.com

Tommaso Sartor is with the MECO Research Team, Department Mechanical Engineering, KU Leuven, Leuven, Belgium {tommaso.sartor}@kuleuven.be

Moritz Diehl is with the Department of Microsystems Engineering (IMTEK) and Department of Mathematics, University Freiburg, 79110 Freiburg, Germany {moritz.diehl}@imtek.uni-freiburg.de

These differential equations arise in: rigid-bodies with friction and impact, electronics, traffic flows, biological systems, economical systems, energy systems, cf. [7].

There are many different formalisms to model nonsmooth dynamic phenomena, for an overview the reader is referred to the excellent monographs [1], [7], [18]. Despite the very good and solid developments both in theory (e.g., existence and uniqueness of solutions for various formalisms [7], [18]) and numerical simulation methods [1], there is still a lack of practical numerical optimal control methods for the three classes of dynamics systems we mentioned. While the first class poses no major obstacle to practical solution, e.g. with smoothing, the second and third classes are difficult and we briefly mention some existing optimal control approaches for them.

The solutions of the second and third class are piecewise smooth. A common approach is to use binary indicator variables for the smooth pieces and apply Mixed Integer Nonlinear Programming (MINLP) [13]. An alternative to MDIs or Differential Variational Inequalities (DVI) of index 2 [14] to model dynamics with state jumps is to use the *hybrid systems* formalism [10]. Thereby, after the trajectories hit the boundary of a *flow set* an algebraic *jump map* is used for the state reinitialization. OCP formulations with this formalism result also in MINLPs [2]. Nonconvex MINLP approaches are often far from being computationally tractable.

A different approach is to determine the order of the smooth pieces/modes in an outer loop with a *mode-scheduling* algorithm and solve a smooth nonlinear program (NLP) where the length of the modes (or stages) is optimized [21]. Besides the fact that mode-scheduling outer loop algorithms ignore the underlying dynamics, they often require some a priori knowledge, e.g., the order of steps for a walking robot [21].

Modeling dynamic systems with different modes (e.g. switched systems) with complementarity conditions (CC) is gaining more popularity [4], [5]. Discretization of Optimal Control Problems (OCP) with CCs results in Mathematical Programs with Complementarity Constraints (MPCC). Walking, running and manipulation problems are rich sources of OCPs with nonsmooth dynamics in robotics [15]. Rigid-body impact problems with friction are naturally modeled with the use of CCs. Thereby, after discretization one also has to solve MPCCs [15]. Many MPCC algorithms use smoothing, relaxation or penalty methods [16]. Conditions for obtaining the right numerical sensitivities with smoothing of differential equations with a discontinuous r.h.s. are provided in the excellent paper by Stewart and Anitescu [19]. Their result

is extended to MPCCs originating from OCPs in [12]. The main conclusion from these works is: in direct collocation for the case 2 of dynamic systems one has to use a sufficiently small step size in comparison with the smoothing parameter, so that the sensitivities of the smoothed system approach the sensitivities of the nonsmooth dynamic system.

A. Contributions and Outline

In this work we present a novel formulation of restitution laws for nonsmooth differential equations with state jumps. The main idea is to introduce an auxiliary dynamic system, where the initial and endpoint of the solution on some interval satisfy the restitution law. Furthermore, a clock state is introduced which does not evolve when the auxiliary dynamic system is active. Finally, we take the pieces of the trajectories corresponding to the time intervals where the clock state is evolving and thereby we recover the solution of the original dynamic system with state jumps. The efficacy of this approach is demonstrated in both simulation and optimal control experiments.

The paper is structured as follows: Section II introduces the main ideas and all terminology, followed by Section III where all concepts are illustrated on a simple example. In Section IV we relate the solutions of the original dynamic system and our formulation and show how to recover the original solution in the general case. Section V provides both simulation and optimal control examples. We compare our approach to a handcrafted multi-stage formulation and get the best solution without the need of stage number enumeration or heuristics. The paper concludes and discusses further extensions in Section VI.

B. Notation

For the time derivative of a function $x(t)$ we use $\dot{x}(t) := \frac{dx(t)}{dt}$ and for $y(\tau)$ we use $y'(\tau) := \frac{dy(\tau)}{d\tau}$. For the left and right limit, we use the notation $x(t_s^+) = \lim_{t \rightarrow t_s, t > t_s} x(t)$ and $x(t_s^-) = \lim_{t \rightarrow t_s, t < t_s} x(t)$, respectively. The matrix $\mathbb{1}_{n,n} \in \mathbb{R}^{n \times n}$ is the identity matrix, and $0_{m,n} \in \mathbb{R}^{m \times n}$ is the zero matrix.

II. TIME-FREEZING OF DIFFERENTIAL EQUATIONS WITH STATE JUMPS

We regard differential equations with unilateral constraints and state jumps: $\dot{x}(t) = f(x(t))$, $\psi(x(t)) \geq 0$. The switching manifold S is defined as $S = \{x \mid \psi(x) = 0\}$ and splits the state space \mathbb{R}^{n_x} into two pieces: the feasible region $V^+ := \{x \mid \psi(x) \geq 0\}$ and the prohibited region $V^- := \{x \mid \psi(x) < 0\}$. Moreover, depending in which direction the trajectory points, and using $\dot{\psi}(x) := \nabla\psi(x)^\top f(x)$, the switching manifold can be split into the following subsets: $S^+ := \{x \mid x \in S, \dot{\psi}(x) > 0\}$, $S^- := \{x \mid x \in S, \dot{\psi}(x) < 0\}$ and $S^0 := \{x \mid x \in S, \dot{\psi}(x) = 0\}$. At time of impact t_s , just before the impact $x(t_s^-) \in S^-$ and the trajectory points outside the feasible region V^+ ($\nabla\psi(x(t_s^-))^\top f(x(t_s^-)) < 0$). To keep the trajectory feasible, a state jump has to occur so that the trajectory points again into V^+ , i.e. $x(t_s^+) \in S^+$.

This is achieved with the restitution law $\Gamma : S^- \rightarrow S^+$. We collect these properties in the following definition:

Definition 1 (Ordinary Differential Equation with State Jumps). *We define the time $t \in \mathbb{R}$ and the differential states $x(t) \in \mathbb{R}^{n_x}$. A system of differential equations with state jumps describes the dynamic evolution of the state vector $x(t)$ as*

$$\dot{x}(t) = f(x(t)), \quad x(t) \in V^+, \quad (1a)$$

$$x(t^+) = \Gamma(x(t^-)), \quad \text{if } \psi(x(t)) = 0 \text{ and } x(t^-) \in S^-, \quad (1b)$$

where $\psi(x(t)) : \mathbb{R}^{n_x} \rightarrow \mathbb{R}$ describes a constraint on the dynamics $f : \mathbb{R}^{n_x} \rightarrow \mathbb{R}^{n_x}$. The function $\Gamma : S^- \rightarrow S^+$ is the restitution law and is used at all t where $x(t) \in S^-$.

In case of mechanical impact problems, such systems are sometimes called *vibro-impact systems* [6]. As an example of such systems we consider the dynamics of a ball bouncing on a table, which is given by:

$$m\dot{v}(t) = -mg, \quad \dot{p}(t) = v(t), \quad \text{if } p(t) \geq 0 \quad (2a)$$

$$v(t^+) = -\gamma v(t^-), \quad \text{whenever } p(t) = 0 \wedge v(t) < 0, \quad (2b)$$

where $p(t)$ is the height of the ball, $v(t)$ is the velocity of the ball, m is the mass of the ball and g is the gravitational acceleration. Equation (2b) is Newton's restitution law for impact dynamics, where $\gamma \in [0, 1]$ is the *coefficient of restitution*. Several other restitution laws can be found in the literature, cf. [6]. The goal of the restitution law is to prevent the ball from penetration (i.e. violating $p(t) \geq 0$).

Since in the general case, the time of impact t is not known a priori, simulating and incorporating such models with additional algebraic conditions into optimization problems is difficult. To alleviate all these difficulties we propose the following approach. First, we relax the constraint $\psi(t) \geq 0$ and define an auxiliary dynamic system on V^- to mimic the restitution law. Second, we introduce a clock state t that evolves according to $t'(\tau) = 1$. The time τ , denoted as *pseudo time* is now the time of the differential equation. The state evolution of $x(\cdot)$ from Definition 1 in pseudo time is denoted as $\tilde{x}(\tau)$. Third, we "freeze" the time whenever $\tilde{x}(\tau) \in V^-$, i.e. $t'(\tau) = 0$. To mimic the restitution law, we assume there exists an auxiliary ODE, whose endpoints satisfy the restitution law on a finite time interval:

Assumption 1. *There exists an auxiliary dynamic system $\tilde{x}'(\tau) = \varphi(\tilde{x}(\tau))$ such that for every initial value $\tilde{x}(\tau_s) = \tilde{x}_0 \in S^-$, the following properties hold on a finite and well-defined time interval (τ_s, τ_r) , (with $\tau_{\text{jump}} := \tau_r - \tau_s$): $\tilde{x}(\tau) \in V^-$, $\forall \tau \in (\tau_s, \tau_r)$, the dynamics have its first intersection with S after τ_{jump} with $\tilde{x}(\tau_r) \in S^+$ and $\tilde{x}(\tau_r) = \Gamma(\tilde{x}(\tau_s))$.*

We collect all the introduced ideas in the following definition:

Definition 2 (Time-Frozen Differential Equations). *We define the pseudo-time $\tau \in \mathbb{R}$, the differential states $y(\tau) := (\tilde{x}(\tau), t(\tau)) \in \mathbb{R}^{n_x+1}$. A system of differential equations describes the dynamic evolution of the state vector $y(\tau)$*

as

$$y'(\tau) = \begin{cases} \tilde{f}(y(\tau)), \tilde{\psi}(y(\tau)) \geq 0, \\ \tilde{\varphi}(y(\tau)), \tilde{\psi}(y(\tau)) < 0, \end{cases} \quad (3a)$$

$$(3b)$$

with $\tilde{f}(y(\tau)) := (f(\tilde{x}(\tau)), 1)$, $\tilde{\varphi}(y(\tau)) := (\varphi(\tilde{x}(\tau)), 0)$ and $\tilde{\psi}(y(\tau)) := \psi(\tilde{x}(\tau))$. It is assumed that Assumption 1 is satisfied.

In the next section we illustrate the ideas and terminology on the example of the bouncing ball.

III. AN ILLUSTRATING EXAMPLE

We consider the dynamics of a ball bouncing on a table given by (2). To mimic the restitution law, whenever $\tilde{p}(\tau) < 0$, we use the following linear ODE for the time interval (τ_s, τ_r) :

$$\tilde{v}'(\tau) = -k\tilde{p}(\tau) - c\tilde{v}(\tau), \quad \tilde{p}'(\tau) = \tilde{v}(\tau), \quad t'(\tau) = 0, \quad (4)$$

The initial values are $\tilde{p}(\tau_s) = 0$, $t(\tau_s) = \tau_s$ and $\tilde{v}(\tau_s)$ has the value of $v(\cdot)$ corresponding to the solution of (2) at τ_s . The first two equations in (4) are a second-order linear ODE and can be solved analytically. Using so-called spring-damper systems to model mechanic impact is an old idea, cf. Chapter 2 in [6]. However, to get realistic approximations of rigid-body impact dynamics the systems has to get "infinitely stiff", which makes it impractical in numerical computations. The key difference here is the introduction of the clock state with time-freezing. As we will see below, this relaxes the requirement of having very stiff dynamics to mimic impacts.

Since $\tilde{v}(\tau_s) < 0$ and $\tilde{p}(\tau_s) = 0$ with the right choice of the parameters k and c in (4), we have $\tilde{v}(\tau_r) > 0$ and $\tilde{p}(\tau_r) = 0$. Afterwards we switch back to the dynamic system defined for $\tilde{p}(\tau) \geq 0$, which is discussed below. For the solution of (4) we require it to satisfy

$$\tilde{v}(\tau_r) = -\gamma\tilde{v}(\tau_s), \quad \tilde{p}(\tau_r) = 0. \quad (5)$$

If $\gamma = 1$ we simply pick some $k > 0$ and set $c = 0$. In the case $\gamma \in (0, 1)$, using the analytic solution of the ODE (4) and assuming $c^2 - 4k < 0$ we can select k and c so that the conditions (5) are satisfied. For a fixed $k > 0$ we can easily derive the following formula for c

$$c = 2|\ln(\gamma)|\sqrt{\frac{k}{\ln(\gamma)^2 + \pi^2}}. \quad (6)$$

As already mentioned, after τ_r we switch back to the initial model with some modifications. Since $\tilde{p}(\tau_r) > 0$ (ball not in contact anymore) we can locally ignore the equation (2b). Furthermore, we add the dynamics of the clock state $t'(\tau) = 1$, thus we get the following ODE:

$$m\tilde{v}'(\tau) = -mg, \quad \tilde{p}'(\tau) = \tilde{v}(\tau), \quad t'(\tau) = 1, \quad (7)$$

Using the compact notation $y(\tau) := (\tilde{p}(\tau), \tilde{v}(\tau), t(\tau))$ and denoting the r.h.s of (7) in compact form as $f_1(y(\tau))$ and analogously the r.h.s. of (4) as $f_2(y(\tau))$, and defining $\tilde{\psi}(y(\tau)) = \tilde{p}(\tau)$, we can write the combined dynamics in compact form as

$$y'(\tau) \in f_1(y)\alpha_0(\tilde{\psi}(y)) + f_2(y)(1 - \alpha_0(\tilde{\psi}(y))), \quad (8)$$

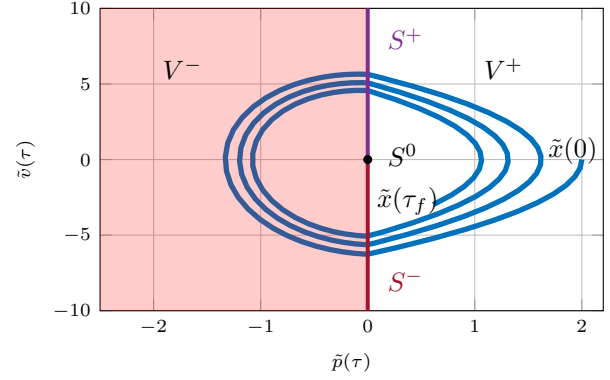


Fig. 1. The state space and phase plot of the time-frozen dynamic system (8). The red shaded area V^- is the prohibited region where the auxiliary dynamic flows and mimics the state jump so that the beginning point of every arc is in S^- and end point in S^+ .

where $\alpha_0(z)$ is a set-valued indicator function such that $\alpha_0(z) = 1$ if $z > 0$, $\alpha_0(z) = 0$ if $z < 0$, and $\alpha_0(z) \in [0, 1]$ if $z = 0$. The inclusion in (8) accounts for the case if the dynamics stays on the manifold $\psi(y(\tau)) = 0$, which does not happen in our case. For more details see the concept of Filippov inclusions [9]. The equation (8) is an example of Definition 2 and the auxiliary dynamic system $y'(\tau) = f_2(y(\tau))$ satisfies all conditions of Assumption 1 by construction. Figure 1 depicts the phase plot of (8).

The set-valued indicator function $\alpha_0(z)$ can be represented as the solution of a parametric linear program (LP) [4]

$$\alpha_0(z) = \underset{w}{\operatorname{argmin}} -zw \text{ s.t. } 0 \leq w \leq 1. \quad (9)$$

Using either the necessary and sufficient conditions of the LP in variational form or its KKT conditions combined with (8), we get a DVI or Dynamic Complementary System (DCS), respectively. We use the latter form for computational reasons, which is discussed in more detail in Section V.

Note that for this formulation we can apply a number of different numerical simulation methods [1], which are not suitable for dynamics with state jumps. Observe that we got rid of the conditional algebraic restitution law (2b). We have in fact a simpler nonsmooth dynamic system than (2), since the solution of (8) is absolutely continuous [9] and contains no jumps. We have in fact reduced the difficult case 3 with jumps to the simpler case 2 without jumps. Hence, there is no need to use measures, which simplifies the theoretical analysis as well as the numerical computation.

After getting rid of the state jump, the question is how to recover the true solution with state jumps? For illustration, we simulate (8) with $\tilde{p}(0) = 10$, $\tilde{v}(0) = 0$ and $t(0) = 0$. We take $\gamma = 0.9$, where for a fixed $k = 20$, we obtain $c = 0.2998$ via (6). Figure 2 depicts the evolution of the clock state $t(\tau)$. We distinguish between three time concepts: 1) the *pseudo time* τ , which is the time of the nonsmooth dynamic system; 2) the *physical time* t , the part of the pseudo time whenever $t'(\tau) > 0$; 3) the *virtual time* t_v , the part of the pseudo time τ whenever $t'(\tau) = 0$ (restitution phases).

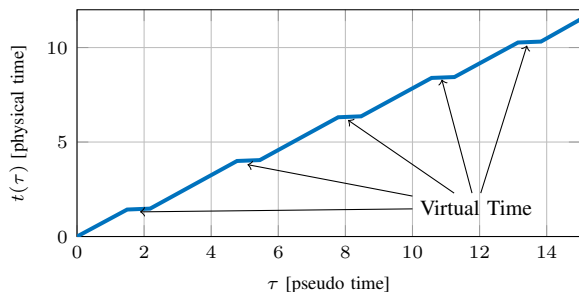


Fig. 2. The clock state $t(\tau)$, with an illustration of the pseudo time, virtual time and physical time. The length of the pseudo time intervals is always the same τ_{jump} .

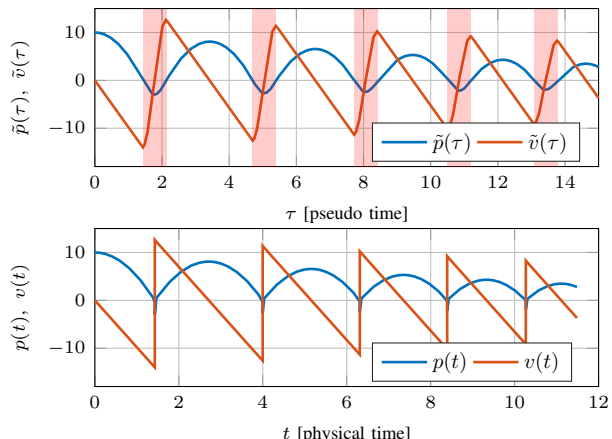


Fig. 3. The velocity $v(\tau)$ and position $y(\tau)$ of the bouncing ball in pseudo time τ (top), and physical time $t(\tau)$ (bottom). The red shaded area in the top plots marks the intervals where the auxiliary dynamic system is active. The top plot in Figure 3 depicts the state trajectories $\tilde{p}(\tau)$ and $\tilde{v}(\tau)$ in pseudo time τ and the bottom plot show the state trajectories in physical time $p(t(\tau))$ and $v(t(\tau))$. Obviously, we recover the true trajectories of the model in (2). The formal proof for this observation in a more general setting is provided in Section IV. Note that if we pick a large k , the system gets more stiff, hence we would need a small step size for accurate simulations, on the other hand this makes the transition faster, so we can select a smaller simulation time τ_f to get to the desired final physical time $t(\tau_f)$. In fact, using the analytic solution of (4) and equation (6), the length of the *restitution phase* τ_{jump} can easily found to be

$$\tau_{\text{jump}} = \sqrt{\frac{\pi^2 + \ln(\gamma)^2}{k}}. \quad (10)$$

Moreover, it is easy to see that in this example with our model we do not obtain Zeno behavior (infinite switches in finite time), since every switch requires some virtual time to perform the state jump, which is upper bounded by the total pseudo simulation time τ_f . The case of an inelastic and persistent contact ($\gamma = 0$) is different and beyond the scope of this paper.

IV. SOLUTION RELATIONSHIP

In this section we show how the solutions of the initial nonsmooth differential equation with a state jump law (1)

and the corresponding time-frozen system (3) are related. Note that the function $t(\tau; x_0)$ is monotone by construction, e.g. Figure 2. Using the definitions from Section II we can state the main theoretical result.

Theorem 1. *Suppose that Assumption 1 holds. Consider the initial value problem (IVP) corresponding to Definition 2 with a given $y_0 = (x_0, 0)$ and $x_0 \in V^+$ on a time interval $(0, \tau_f)$, and the IVP corresponding to Definition 1 with the initial value x_0 on a time interval $(0, t_f) := (0, t(\tau_f))$. Suppose that we have at most one time point t_s where $\psi(x(t_s)) = 0$ on the time interval $(0, t_f)$. Then the solution of the two IVPs: $x(t; x_0)$ and $y(\tau; y_0)$ fulfill at any $t \neq t_s$*

$$x(t(\tau)) = Ey(\tau), \quad (11)$$

with

$$E = \begin{bmatrix} \mathbb{1}_{n_x, n_x} & 0_{n_x, 1} \\ 0_{1, n_x} & 0 \end{bmatrix}.$$

Proof: Denote the solution of IVP given by (3a) and y_0 as $y_1(\tau; y_0)$ for some $\tau \in (0, \hat{\tau})$. Similarly, for (1a) and $x_0 \in V^+$ for some $t(\tau) \in (0, t(\hat{\tau}))$ as $x_1(t(\tau); x_0)$. Note that if there is no $t_s \in (0, t_f)$ such that $\psi(x(t_s)) = 0$ on this interval, then $t(\tau) = \int_0^\tau d\tau_1 = \tau$. Then setting $\hat{\tau} = \tau_f$, relation follows that (11), since due to Definitions 1 and 2 it follows $x_1(t; x_0) = x(t; x_0)$ and $y_1(\tau; y_0) = y(\tau; y_0)$.

If we have some $t_s \in (0, t_f)$ so that $\psi(x(t_s)) = 0$, then from the first part of the proof we have that (11) holds for all $\tau \in (0, \tau_s^-)$ and hence for all $t(\tau) \in (0, t_s^-)$, with $t_s = \tau_s$. Its only left to prove that (11) holds for $\tau \in (\tau_s^+, \tau_f)$ and the respective $t(\tau)$. Due to Assumption 1 there exists a dynamic system $\tilde{x}'(\tau) = \varphi(\tilde{x}(\tau))$ that satisfies the restitution law and we have that $y(\tau_r; y_0) = \Gamma(y(\tau_s; y_0)) = y_s$. Note that $t'(\tau) = 0$ with $\tau \in (\tau_s, \tau_r)$, hence $t(\tau_r) = t(\tau_s) = t_s$. Using this we have $y_1(\tau - \tau_r, y_s) = y(\tau, y_0)$ for $\tau \in (\tau_r, \tau_f)$ and with denoting $x_s = Ey_s$, we see that $x_1(t(\tau) - t_s; x_s) = x(t(\tau), x_0)$ for $t(\tau) \in (t_s^+, t_f)$. Since the intervals (t_s, t_f) and (τ_r, τ_f) have the same length and $x_s = Ey_s$, from the definitions of the corresponding IVPs, the relation (11) holds. This completes the proof. \square

The assumptions that we have at most one state jump on the time interval $(0, t_f)$ can be always satisfied by shortening the regarded time interval and simplifies the proof without loss of generality. Furthermore, we avoid the analysis of the case with infinite switches in finite time (Zeno behavior). For a desired physical simulation t_f we always have to take a longer pseudo simulation time $\tau_f = t_f + N_J \tau_{\text{jump}}$ where N_J is the number of state jumps on $(0, t_f)$ for the original system. Obviously, we do not know a priori the number N_J . However, in OCPs this can be easily overcome with the use of a time transformation, which is shown in the next section.

V. NUMERICAL EXAMPLES

A. Numerical Simulation

We first demonstrate the ease of use of the time-freezing in simulation problems. Consider again the example from Section III. The initial value is set to $x(0) = (0.5, 0)$ and

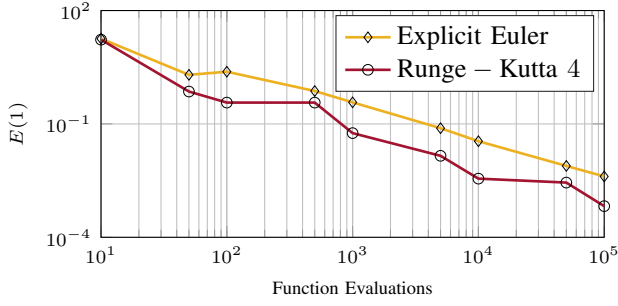


Fig. 4. Accuracy of the explicit Euler scheme and Runge-Kutta 4 for different number of function evaluations for the time-freezing reformulation.

we simulate the original system for $t_f = 1$ s. For the time-freezing reformulation we take the compact form of (8) and use the indicator function $\alpha_0(z) = (1 + \text{sign}(z))/2$. In this example the restitution coefficient is picked to be $\gamma = 0.9$, and for $k = 4\pi$ we calculate $c = 0.2376$ via (6). The analytical solution has two jumps during the considered time interval. The pseudo simulation time is set to $\tau_f = 1 + 2\tau_{\text{jump}}$, where $\tau_{\text{jump}} = 0.8867$ and is obtained with equation (10). In this numerical experiment we use the explicit Euler and Runge-Kutta 4 (RK4) schemes. The terminal numerical error, denoted as $E(1) = \|x(1) - \tilde{x}(t(\tau_f))\|_2$ is plotted over the number of function evaluations M in the integrator, see Figure 4. We clearly see that the error decreases for both methods with a smaller step size and that the numerical time-freezing solution converges to the analytic solution, which also confirms the result of Theorem 1. Due to the remaining nonsmoothness (case 2), the RK4 method does only achieve an order of one, as the Euler method. Opposed to standard spring-damper impact models, the most notable observation for our reformulation is that we do not need a large k (which makes the system very stiff and costly to integrate) to get a very accurate numerical approximation.

B. Numerical Optimal Control

To demonstrate the ease of use and benefits of the time-freezing reformulation, we consider an OCP with the bouncing-ball dynamics. We apply a magnetic force $F \in [-mg, mg]$ and the goal is: starting at $p(0) = 0.5$ m, to have the ball after $T = 3$ s at $p(T) = 1$ m, while minimizing the integral of the squared force.

1) *Multistage Formulation:* For comparison 1) we consider a multistage formulation. We prescribe the number of jumps $N_J \geq 1$ and at the end of every stage, we impose the restitution law (2b). Essentially, this problem consists of N_J OCPs which are linked together. Moreover, we apply a time transformation to every stage to handle different lengths of the free flight stages. Thereby, in every stage, the time t_i is replaced by $t_i = w_i \tau_i$ with $\tau_i \in [0, 1]$, the dynamics is augmented with the clock state $t'_i(\tau_i) = w_i$ (not to be confused with the clock state in time-freezing, the r.h.s is smooth here). All time derivatives are now with respect to τ_i and w_i is a parameter. The states are $x_i := (y_i, v_i, t_i)$ for all $i = \{1, \dots, N_J\}$ and the initial value is $x_0 = (0.5, 0, 0)$. We

omit for brevity the full statement of the multi-stage OCP, for more details see Chapter 9 in [8]. We also have an upper and lower bound on $w_i \in [w_{\text{max}}^{-1}, w_{\text{max}}]$ with $w_{\text{max}} = 20$, to avoid numerical difficulties. This OCP is discretized with the use of direct collocation [17] and thereby we use a Gauss-Legendre scheme of order 4 with a step size of $h = 0.0025$ for every stage. The discretized control inputs are taken to be constant over the finite elements. Observe that to keep the step size h constant, the number of optimization variables increases as we increase N_J . The discretized OCP is solved with IPOPT [20] via its CasADi [3] interface in MATLAB. With enumerating N_J from 1 to 10, we found the best objective for $N_J = 4$ with a value of 4.2362.

2) *Time-Freezing Formulation:* Now we formulate an OCP with the same objective and constraints, however the dynamics are give by the time-freezing reformulation. The OCP reads as:

$$\min_{x(\cdot), F(\cdot), w} \int_0^1 wF(s)ds \quad (12a)$$

$$\text{s.t.} \quad x(0) - x_0 = 0, \quad (12b)$$

$$v'(s) \in w[\alpha_0(p(s))(-g + F/m) + (1 - \alpha_0(p(s)))(-cv(s) - kp(s))], \quad (12c)$$

$$p'(s) \in w\alpha_0(p(s))v(s), \quad (12e)$$

$$t'(s) \in \alpha_0(p(s))w, \quad (12f)$$

$$-mg \leq F(s) \leq mg, \quad (12g)$$

$$w_{\text{max}}^{-1} \leq w \leq w_{\text{max}}, \quad (12h)$$

$$t(1) = T. \quad (12i)$$

In this OCP also a time transformation $\tau = ws$ is used, where w is a parameter (the "speed of pseudo-time") and s is the new pseudo-time. All time-derivatives are now w.r.t. s , hence all differential equations are scaled by w . For an initial guess for w we set $2T$ as it is likely to be greater than T since the auxiliary dynamics take some of the "time budget". In the dynamics (12d) we replace the indicator function $\alpha_0(y(s))$ with the KKT conditions from the parametric LP formulation (9) and get a DCP, cf. [12]. As in the multi-stage case we use a fully simultaneous approach with direct collocation and discretize the infinite-dimensional OCP using the Gauss-Legendre scheme with order 4 and step size $h = 0.0025$. The discretized control inputs are taken to be constant over the finite elements. Since we discretize a DCP the discretized OCP yields an NLP which is an MPCC. To solve the OCP we will relax the complementarity constraints with a positive parameter $\sigma > 0$ (e.g. $a \circ b = 0$ is replaced with $a \circ b \leq \sigma$) and obtain a smooth NLP after discretization. To solve an MPCC originating from an OCP, special care has to be taken. In [12] it was shown that in discretized OCPs resulting in MPCCs, we have to take a step size $h = o(\sigma)$ to get the right numerical sensitivities and avoid getting stuck in spurious local solutions close to the initial guess. In the homotopy approach, we solve a sequence of NLPs and the parameter σ is updated with the following rule: $\sigma_{i+1} = 0.4\sigma_i$, with $\sigma_0 = 10$, where i is the number of the problem in the sequence.

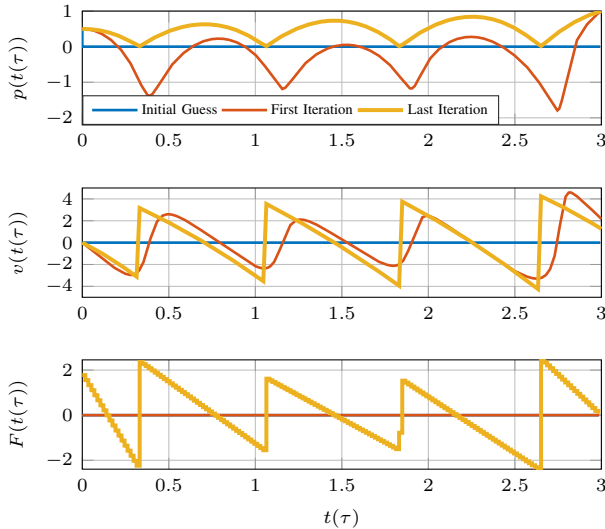


Fig. 5. The position $p(t(\tau))$ (top), velocity $v(t(\tau))$ (middle) and control force $F(t(\tau))$ bottom in physical time $t(\tau)$. The plots shows three trajectories: the initial solution guess (blue), after the first homotopy iteration (red) and the solution (yellow).

The primal solution of the previous problem is used as a solution guess for the next problem in the sequence and we solve in this example in total 11 problems, again with IPOPT [20] via its CasADi [3] interface.

With our approach we get the same solution as the best multi-stage solution with $N_J = 4$ and an objective value of 3.9989^1 , without the need of specifying the number of stages (which in some examples might become arbitrarily complex). Figure 5 depicts the numerical OCP solution as well as the initial guess and the result after first homotopy iteration. Interestingly, the number of jumps is found after the first iteration, and in the remainder the algorithm finds the right control inputs and gets a numerically accurate solution. There is no need for integer variables, nor for a good solution guess, nor the need to incorporate the restitution law explicitly (it is not even clear how this could be done in a smooth optimization problem formulation). Furthermore, we can use the efficient smoothing and relaxation methods to handle the dynamics with state jumps in OCPs. Observe that if many switches occur, w has to take a larger value so the terminal physical time T can be reached, since every restitution phase “uses” a part of the available pseudo time. This might require one to use a smaller step size h to achieve the desired accuracy.

VI. CONCLUSIONS AND OUTLOOK

In this paper we proposed a novel reformulation for differential equations with state jumps into a significantly easier class of problems. We also provide a proof that the solutions of the two systems are related and how to recover the solution of the original system. The proposed reformulation

¹Note that we solve a nonconvex NLP and in general one cannot expect to find always the global optimum. The difference in the objective is due to smoothing and effectively a different step size h .

significantly simplifies to use differential equations with state jumps in numerical optimal control. The efficacy of the approach is illustrated on a simulation example and one optimal control problem where we get the same solution as the best solution of a carefully hand crafted multi-stage formulation. The hard part, in general, is how to determine the auxiliary dynamic system in Assumption 1, so that a given restitution law is satisfied. A systematic way to obtain such a differential equation is subject of future research.

REFERENCES

- [1] Vincent Acary and Bernard Brogliato. *Numerical methods for nonsmooth dynamical systems: applications in mechanics and electronics*. Springer Science & Business Media, 2008.
- [2] Berk Altun, Pegah Ojaghi, and Ricardo G Sanfelice. A model predictive control framework for hybrid dynamical systems. *IFAC-PapersOnLine*, 51(20):128–133, 2018.
- [3] Joel A. E. Andersson, Joris Gillis, Greg Horn, James B. Rawlings, and Moritz Diehl. CasADi: a software framework for nonlinear optimization and optimal control. *Mathematical Programming Computation*, 2018.
- [4] B.T. Baumrucker and L.T. Biegler. MPEC strategies for optimization of a class of hybrid dynamic systems. *Journal of Process Control*, 19(8):1248–1256, 2009.
- [5] Hans Georg Bock, Christian Kirches, Andreas Meyer, and Andreas Potschka. Numerical solution of optimal control problems with explicit and implicit switches. *Optimization Methods and Software*, 33(3):450–474, 2018.
- [6] Bernard Brogliato. *Nonsmooth Mechanics: Models, Dynamics and Control*. Springer, 2016.
- [7] Bernard Brogliato and Aneel Tanwani. Dynamical systems coupled with monotone set-valued operators: Formalisms, applications, well-posedness, and stability. *SIAM Review*, 62(1):3–129, 2020.
- [8] Moritz Diehl and Sebastien Gros. *Numerical Optimal Control*. –, expected to be published in 2018.
- [9] Aleksei Fedorovich Filippov. *Differential equations with discontinuous righthand sides: control systems*, volume 18. Springer Science & Business Media, 2013.
- [10] R. Goebel, R.G. Sanfelice, and A.R. Teel. Hybrid Dynamical Systems. *IEEE Control Systems Magazines*, 29(2):28–93, April 2009.
- [11] Jean Jacques Moreau. Evolution problem associated with a moving convex set in a Hilbert space. 1977.
- [12] Armin Nurkanović, Sebastian Albrecht, and Moritz Diehl. Limits of MPCC Formulations in Direct Optimal Control with Nonsmooth Differential Equations. In *Proceedings of the European Control Conference (ECC) 2020*, 2020.
- [13] J. Oldenburg. *Logic-based modeling and optimization of discrete-continuous dynamic systems*, volume 830 of *Fortschritt-Berichte VDI Reihe 3, Verfahrenstechnik*. VDI Verlag, Düsseldorf, 2005.
- [14] Jong-Shi Pang and David E Stewart. Differential variational inequalities. *Mathematical Programming*, 113(2):345–424, 2008.
- [15] Michael Posa, Cecilia Cantu, and Russ Tedrake. A direct method for trajectory optimization of rigid bodies through contact. *The International Journal of Robotics Research*, 33(1):69–81, 2014.
- [16] Daniel Ralph* and Stephen J Wright. Some properties of regularization and penalization schemes for mpecs. *Optimization Methods and Software*, 19(5):527–556, 2004.
- [17] J. B. Rawlings, D. Q. Mayne, and M. M. Diehl. *Model Predictive Control: Theory, Computation, and Design*. Nob Hill, 2nd edition, 2017.
- [18] David E Stewart. *Dynamics with Inequalities: impacts and hard constraints*, volume 59. SIAM, 2011.
- [19] David E Stewart and Mihai Anitescu. Optimal control of systems with discontinuous differential equations. *Numerische Mathematik*, 114(4):653–695, 2010.
- [20] Andreas Wächter and Lorenz T. Biegler. On the implementation of an interior-point filter line-search algorithm for large-scale nonlinear programming. *Mathematical Programming*, 106(1):25–57, 2006.
- [21] Alexander W Winkler, C Dario Bellicoso, Marco Hutter, and Jonas Buchli. Gait and trajectory optimization for legged systems through phase-based end-effector parameterization. *IEEE Robotics and Automation Letters*, 3(3):1560–1567, 2018.